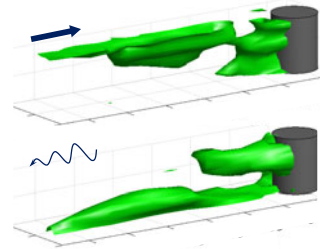


Three-dimensional viscoelastic instabilities in microchannels

R. J. Poole[†]

School of Engineering, University of Liverpool,
Brownlow Hill, Liverpool, L69 3GH, UK



Whereas the flow of simple single-phase Newtonian fluids tends to become more complex as the characteristic length scale in the problem (and hence the Reynolds number) increases, for complex elastic fluids such as dilute polymer solutions the opposite holds true. Thus small-scale, so-called ‘microfluidic’ flows of complex fluids can exhibit rich dynamics in situations where the ‘equivalent’ flow of Newtonian fluids remains linear and predictable. In the recent study of Qin *et al.* (*J. Fluid Mech.*, vol. 864, 2019, R2) of the flow of a dilute polymeric fluid past a 50 μm cylinder (in a $100 \times 60 \mu\text{m}$ channel), a novel 3-D holographic particle velocimetry technique reveals the underlying complexity of the flow, including inherent three-dimensionality and symmetry breaking as well as strong upstream propagation effects via elastic waves.

Key words: polymers, viscoelasticity

1. Introduction

Purely elastic instabilities (Shaqfeh 1996) driven by elastic normal stresses have been widely observed in the absence of significant inertial effects, in both viscometric flows, that imparts steady shearing motion on each fluid particle (Larson, Shaqfeh & Muller 1990), and more general non-viscometric flow geometries (Pakdel & McKinley 1996). In addition to the usual material properties of density ρ and dynamic viscosity η which characterise single-phase Newtonian flows, dilute polymeric solutions, like those used by Qin *et al.* (2019) and most other studies in this area, are also characterised by a ‘relaxation’ time (Bird, Armstrong & Hassager 1987). The Deborah number De , which is a measure of this relaxation time relative to a characteristic residence time of the flow, must become unimportant in fully developed, steady viscometric flows as the characteristic residence time tends to infinity. The second parameter governing the flow of single-phase viscoelastic fluids in the inertialess limit is the Weissenberg number Wi , the ratio of elastic to viscous stresses. These two parameters are often thought of as essentially interchangeable although, in general, they represent subtly different properties of the flow: one quantifying inherently Lagrangian unsteady effects (De) and the other the ‘strength’

[†] Email address for correspondence: robpoole@liverpool.ac.uk

of the flow (Wi). In the problem studied by Qin *et al.* (2019) of flow past a cylinder of diameter d in an approximately square channel of height H , the characteristic time scale of the flow can be estimated as the time taken for a fluid particle to circumvent half the cylinder (i.e. $\pi d/2U \sim d/U \sim H/U$ as $d \sim H$). The Deborah number is then $De \sim \lambda U/H$. The Weissenberg number in Qin *et al.* (2019) is $Wi = N_1/2\tau = N_1/(2\dot{\gamma}\eta)$, where N_1 is the first-normal stress difference (the ‘elastic’ stress), τ the shear stress and $\dot{\gamma}$ the shear rate. Only for an upper-convected Maxwell model (Bird *et al.* 1987), where $N_1 = 2\lambda\eta\dot{\gamma}^2$ and $\tau = \eta\dot{\gamma}$ in steady simple shear, does this yield $Wi = \lambda\dot{\gamma} \sim \lambda U/H$ and hence $Wi = De$. However, De and Wi both increase with decreasing characteristic length scale(s). Hence, the microfluidic environment, which typically minimises inertial effects due to its small length scales, also enhances elastic effects. As a result, microfluidic experiments have been widely exploited to probe purely elastic instabilities in viscoelastic fluids, which usually arise from the combination of elastic stresses and streamline curvature. This mechanism is captured in the phenomenological criterion due to Pakdel & McKinley (1996), which states that instability may arise when the product of a ‘local’ De based on a length scale involving the local streamline curvature (\mathfrak{R}) and a ‘local’ Wi based on local shear rate and local tensile (normal) stress along the streamline exceeds a critical parameter (M_{CR}^2) (i.e. $(N_1/\tau)(\lambda U/\mathfrak{R}) > M_{CR}^2$).

Purely elastic instabilities and, at higher flow rates, even highly disordered flows termed ‘elastic turbulence’ have been observed in a wide range of different geometries. One way of categorising these flows is via a schematic representation – a ‘map’ – demarcating these flows into: viscometric, shear-dominated, extension-dominated and those of mixed kinematics, as shown in figure 1. The map highlights the interrelation between flows of apparently differing character – between the ‘cross-slot’ and the ‘mixing-separating’ geometry, for example, or the similarity between flow past a cylinder and into a contraction. The flow past a cylinder in a channel studied by Qin *et al.* (2019), shown schematically as an inset in figure 1, falls into the island of ‘mixed kinematics’.

2. Overview

Following on from earlier seminal work in the same group by Pan *et al.* (2013), where an array of cylinders in a microfluidic channel was used to show that a sustained elastic instability leading to elastic turbulence could also be achieved in the absence of streamline curvature far downstream of the array, the recent study of Qin *et al.* (2019) looks in detail at the instability around a single cylinder. It is precisely these ‘finite amplitude’ perturbations (Morozov & van Saarloos 2007) which – when combined in an array of cylinders – were able to drive a self-sustaining turbulent motion far downstream (~ 400 channel widths) in the straight channel. Hence an understanding of the underlying instability mechanisms around an isolated cylinder is potentially of broad interest. The significant advance of Qin *et al.* (2019) on most previous studies of purely elastic instabilities (with limited exceptions such as the study by Afik & Steinberg 2017) is in the use of a novel in-line three-dimensional (3-D) holographic particle tracking technique. The technique, detailed in Salipante, Little & Hudson (2017), involves recording using a high-speed camera of the flow seeded with tracer particles and illuminated by a laser mounted on an inverted microscope. In this manner, the positions of the particles are determined using back-scattering reconstruction and a fully 3-D velocity field can be reconstructed by differentiating Lagrangian particle trajectories. These 3-D velocity fields reveal much

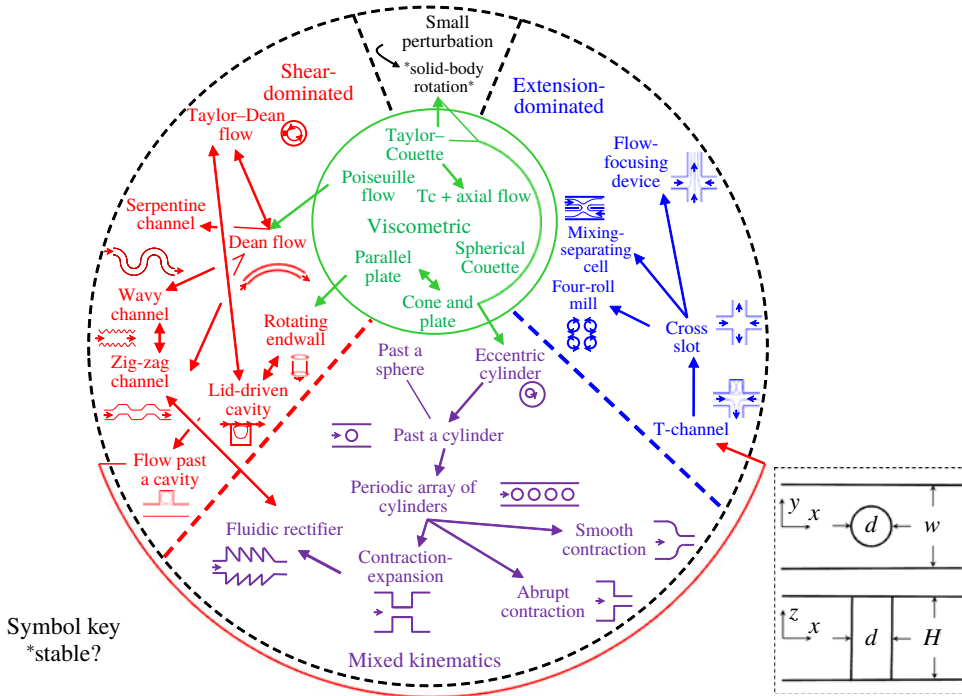


FIGURE 1. Purely elastic flow instability map (‘PEFIM’): a taxonomy for purely elastic instabilities based on flow type, including potential relationships between different prototype geometries. Inset in bottom right-hand corner defines axes for the situation studied by Qin *et al.* (2019).

more complex flow transitions as the flow rate (and hence Wi) is increased than could previously be inferred from two-dimensional measurements. In particular, the findings of Qin *et al.* (2019) of strong three-dimensionality at higher flow rates are significant in that they are likely to be systemic to most microfluidic flows studied to date because most microfluidic channels have finite depth, with an approximately square cross-section (as in Qin *et al.* 2019).

Two-dimensional measurements in the xy -centreplane (see inset of figure 1 for axis definition) of Qin *et al.* (2019) reveal that an upstream vortex develops immediately in front of the cylinder as Wi is increased. Beyond a critical $Wi \sim 4$, the vortex begins to fluctuate weakly in time although it retains its symmetry about the midline of the xy -centreplane. This symmetry is lost beyond $Wi \sim 8$, and for $Wi > 9$ the flow enters a stronger time-dependent regime where the length of the upstream vortex frequently collapses to $\sim 2d$ and then regenerates (up to $6d$).

The novel 3-D measurements reveal that the ‘top’ and ‘bottom’ walls play a fundamental role in the dynamics as the flow at high Wi is revealed to be made up of a pair of separate recirculation zones, each originating between the ‘corner’ of the cylinder and the top/bottom walls. These zones are anticorrelated in that as one grows the other decays – and *vice versa*. Thus symmetry breaking first noted across the midline of the xy -centreplane is followed by symmetry breaking across the midline of the xz -centreplane, and the flow is strongly 3-D, something which is only fully revealed by these new measurements. Finally, the results also suggest the presence of apparently different instability mechanisms upstream and downstream of

the cylinder. The upstream propagation of disturbances suggests that perturbations may be transmitted against the primary flow direction via an ‘elastic wave’, but with a wave speed which does not simply scale with λ . For a viscoelastic shear wave, based on a Maxwell type model with constant polymeric viscosity η_p and relaxation time λ , the wave speed is constant $c_s = \sqrt{(\eta_p/\rho\lambda)}$ and this leaves open precisely what is the physical interpretation of the wave (see also Varshney & Steinberg 2019).

3. Future

Given that the results of Qin *et al.* (2019) reveal the potentially strong influence of the walls on the time-dependent flow which develops, an obvious next step would be to investigate the effect of varying the depth aspect ratio of the channel to determine if this instability always arises at the same preferential location or if new mechanisms arise when the channel is deeper. Novel fabrication methods which allow much higher aspect ratios (for example, Haward, Toda-Peters & Shen 2018) than conventional PDMS microchannels may prove fruitful in this regard. Studies which can probe systematically the effect of varying the viscoelastic shear wave speed, perhaps by changing the polymeric viscosity contribution whilst holding the density and relaxation time approximately constant, may shed more light on the upstream propagation mechanisms. In this vein, and given the rich dynamics observed, fully resolved 3-D time-dependent numerical simulations using viscoelastic constitutive equations would also seem like an interesting avenue to pursue. In this latter case, the simulations have the ability to fully ‘turn off’ inertia, something that a real experiment can never truly do. However, the very complicated flow patterns and dynamics observed experimentally present a significant challenge for numerical simulations and a stringent test of existing viscoelastic constitutive equations.

References

- AFIK, E. & STEINBERG, V. 2017 On the role of initial velocities in pair dispersion in a microfluidic chaotic flow. *Nat. Commun.* **8** (1), 468.
- BIRD, R. B., ARMSTRONG, R. C. & HASSAGER, O. 1987 Dynamics of polymeric liquids. In *Fluid Mechanics*, vol. 1, 2nd edn. Wiley.
- HAWARD, S. J., TODA-PETERS, K. & SHEN, A. Q. 2018 Steady viscoelastic flow around high-aspect-ratio, low-blockage-ratio microfluidic cylinders. *J. Non-Newtonian Fluid Mech.* **254**, 23–35.
- LARSON, R. G., SHAQFEH, E. S. G. & MULLER, S. J. 1990 A purely elastic instability in Taylor–Couette flow. *J. Fluid Mech.* **218**, 573–600.
- MOROZOV, A. N. & VAN SAARLOOS, W. 2007 An introductory essay on subcritical instabilities and the transition to turbulence in visco-elastic parallel shear flows. *Phys. Rep.* **447** (3–6), 112–143.
- PAKDEL, P. & MCKINLEY, G. H. 1996 Elastic instability and curved streamlines. *Phys. Rev. Lett.* **77** (12), 2459–2462.
- PAN, L., MOROZOV, A., WAGNER, C. & ARRATIA, P. E. 2013 Nonlinear elastic instability in channel flows at low Reynolds numbers. *Phys. Rev. Lett.* **110** (17), 174502.
- QIN, B., SALIPANTE, P. F., HUDSON, S. D. & ARRATIA, P. E. 2019 Upstream vortex and elastic wave in the viscoelastic flow around a confined cylinder. *J. Fluid Mech.* **864**, R2.
- SALIPANTE, P. F., LITTLE, C. A. E. & HUDSON, S. D. 2017 Jetting of a shear banding fluid in rectangular ducts. *Phys. Rev. Fluids* **2** (3), 033302.
- SHAQFEH, E. S. G. 1996 Purely elastic instabilities in viscometric flows. *Annu. Rev. Fluid Mech.* **28** (1), 129–185.
- VARSHNEY, A. & STEINBERG, V. 2019 Elastic Alfvén waves in elastic turbulence. *Nat. Commun.* **10**, 652.